

# COMPARISON OF NORMAL CONDUCTING HIGH ENERGY ACCELERATING STRUCTURES FOR A MODERATE OPERATING FREQUENCY \*

V. Paramonov <sup>†</sup>, INR of the RAS, Moscow, 117312, Russia

## Abstract

The progress in the CERN Linac 4 project confirms the very attractive possibility for single frequency high intensity high energy normal conducting hadron linac. The important part of such linac is the accelerating structure for high energy part. The set of parameters, such as dimensions, RF efficiency, field stability, cooling capability, vacuum conductivity, is considered and compared for possible accelerating structures at operating frequency 352 MHz are in proton energy range up to 600 MeV.

## INTRODUCTION

For the high energy part of normal conducting intense hadron linac the Coupled Cell Structure (CCS) is used. For operating frequency  $f_0 = 352.2\text{MHz}$ ,  $\lambda = 85.12\text{cm}$  application of such well known and proven CCS's as the Side Coupled Structure (SCS), the Annular Coupled Structure (ACS) and the Disk And Washers (DAW) is not practical due to enormously large transverse dimensions  $2R_c \sim 1.5\lambda$ . Structures with the smaller outer diameter  $2R_c \sim 0.7\lambda$  look realistic. During TRISPAL project, see [1], LEP-type structure was suggested to take the beam to high energy part. Also consideration of the compact On Axis Coupled (OAS) structure was rejected due low value of the effective shunt impedance  $Z_e$  for low  $\beta$  and possibility of multipactor in coupling cells. This suggestion is successfully developed now and realized in the Pi Mode Accelerating Structure (PiMs) for Linac 4, [2]. The small transverse dimensions has also the Cut Disk Structure (CDS), [3]. Below PiMS and CDS parameters are compared for proton energy range from 50 MeV to 600 MeV.

## PARAMETERS COMPARISON

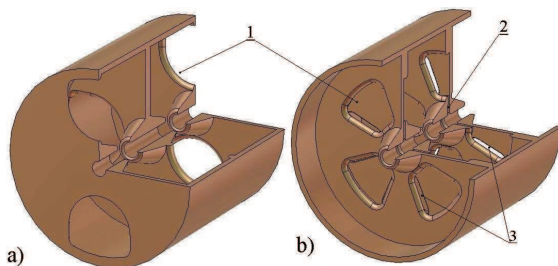


Figure 1: The considered structures, PiMS (a) and CDS (b). 1 - coupling windows, 2- coupling CDS cell, 3 - slots 'To Look Through' (TLT) between CDS cells.

The considered structures are shown in Fig. 1.

## Cells Parameters

For both structures the dimensions of Drift Tube (DT) are essential. Especially interesting is the value of a cone angle  $\theta$  for DT. In PiMS the dimensions of coupling windows are well matched with DT dimensions and cone angle is fixed to  $\theta = 20^\circ$ , [4]. For the energy range from 160 MeV to 600 MeV this value is conserved to provide appropriate dimensions of coupling windows for the higher value of the coupling coefficient  $k_c$ . As it is known well, the optimal for the maximum of  $Z_e$ , length of accelerating gap  $l_g$  depends on  $\theta$ . All time in simulations below for each  $\theta$  the optimal  $l_g$  value was used. Also structures were compared for the same aperture radius.

In CDS another concept of coupling is realized, [3], and there are no essential relationships between  $\theta$  and  $k_c$ . Plots of some CDS parameters in the dependence on  $\theta$  value are shown in Fig. 2. Blue and green lines corresponds to proton energy 100 MeV and 400 MeV, respectively. With  $\theta$  increas-

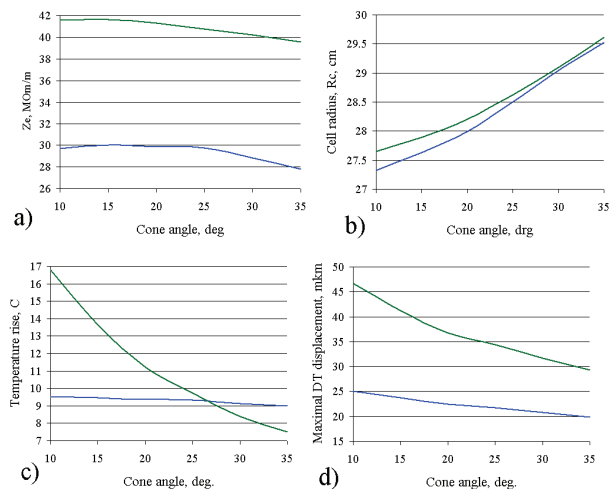


Figure 2: The plots of  $Z_e(\theta)$ , (a),  $R_c(\theta)$ , (b),  $dT_{max}(\theta)$ , (c),  $dz_{max}(\theta)$ , (d) for CDS.

ing to  $\theta \geq 25^\circ$  there is visible  $Z_e$  decreasing, especially for higher energy, and the rise in the cell diameter, Fig. 2a,b. In Fig. 2c,d are shown plots for the maximal temperature rise  $dT_{max}$ , which is realized at the DT tip, and the corresponding increasing in the DT length,  $dz_{max}$ . (See below about CCS cooling). With the small  $\theta \sim (15^\circ \div 20^\circ)$  we have the thin long DT, especially for higher energies. For design simplification, inside DT body there are no cooling channels. Simultaneously, near DT pedestal (in both structures) the

\* Work supported by IHEP contract N 0348100096313000178

<sup>†</sup> paramono@inr.ru

high density of RF losses is realized. The high temperature can be achieved at the DT tip, where the maximal value of electric field takes place. As the compromise, for CDS  $\theta = 25^\circ$  is fixed for further consideration.

The outer CDS vicinity, Fig. 1b, differing from [5], is considered without rounded part. It leads both to acceptable  $Z_e$  reduction at  $(3 \div 4)\%$  and  $R_c$  reduction at  $(2 \div 3)cm$ .

**RF Efficiency**

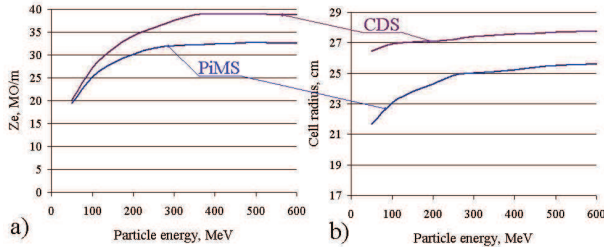


Figure 3: The plots of shunt impedance  $Z_e$ , (a), and cell radius  $R_c$ , (b), for PiMS and CDS.

In Fig. 3 are shown the plots of  $Z_e$  and cell radius  $R_c$  for PiMS and CDS in dependence on proton energy. Both structures have practically the same ratio  $\frac{Z_e}{Q}$  and plots of quality factor  $Q$  are very similar to  $Z_e$  ones.

In CCS with coupling slots (windows) the maximal density of RF current  $I_{RFmax}$  is realized at the slots (windows) ends. All time for  $\pi$  structure (PiMS) the maximal  $I_{RFmax}$  value is  $\approx 2$  times higher, as compared to  $\frac{\pi}{2}$  structure (CDS), [3]. It results in much higher ( $\approx 4$  times) density of RF losses at the slots (windows) ends. In Fig. 4 are shown the distribution of RF losses density at the surface of CDS cell (a) and in the common scale comparison of RF losses density for CDS and PiMS for the same accelerating rate. As one can see from Fig. 4b, CDS has much more uniform distribution of RF losses density and it results in higher  $Z_e$  and  $Q$  values.

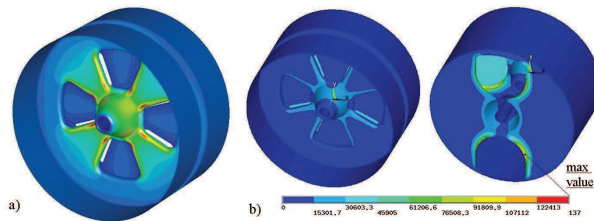


Figure 4: The distribution of RF losses density  $P_{ds}$  at CDS surface (a) and  $P_{ds}$  comparison between CDS and PiMS, (b).

**Structures Cooling**

Cooling conditions are considered both for PiMS and for CDS assuming application in intense linac with a significant heat loading to the structure, corresponding to operation with accelerating rate  $2 \frac{MV}{m}$  and duty factor 6%. The cooling scheme for PiMS is accepted as in [4]. Only drilled channels in the web between cells are foreseen, Fig. 5c,d.

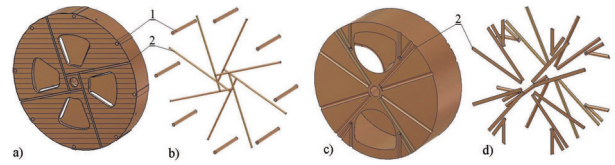


Figure 5: The placement and the scheme of cooling channels for CDS, (a,b) and for PiMS, (c,d)

For CDS, together with drilled internal channels in the web, there are external channels, Fig. 5a,b. Such scheme for CDS provides more uniform DT cooling, [5]. The same diameter for cooling channels and flow velocity  $\approx 2m/sec$  are assumed for both structures. The maximal surface temper-

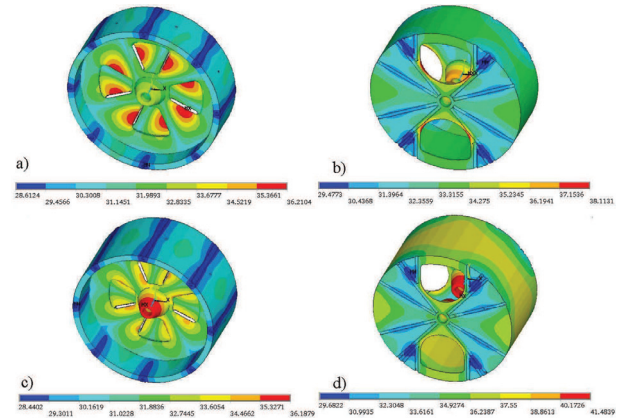


Figure 6: The temperature distributions in CDS cells, (a,c) and PiMS, (b,d) for particles energy 100MeV, (a,b) and 400MeV, (b,d).

ature for PiMS is realized at the drift tube, Fig. 6. In the Table 1 are summarized results for thermal stress analysis for both structures, performed with ANSYS software. In the

Table 1: Thermo-mechanical Effects

Structure	PiMS	PiMS	CDS	CDS
Energy, MeV	100	400	100	400
$dT_{max}, C^\circ$	11.1	14.5	9.2	9.2
$\delta f_a, kHz$	-55.7	-80.3	-67.7	-51.8
$\delta f_c, kHz$	-	-	-339.6	-321.1
$\frac{\sigma_{max}}{E_m}, \%$	0.01	0.09	0.01	0.14

shift of operating frequency  $\delta f_a$  both structures are equal approximately. For CDS there is a significant shift for the frequency for the coupling mode  $\delta f_c \sim 10^{-3} f_0$ . It can be compensated by special pre-tuning of CDS, [6]. The maximal value of internal stress for both structures is expected in the safe limits.

**Coupling, Field Stability, Tuning**

The plots of coupling coefficient  $k_c$  for CDS and PiMS together with calculated dispersion curves are shown in Fig. 7. The natural  $k_c$  decreasing with particle energy for both structures is due to cell length increasing and relative reduction

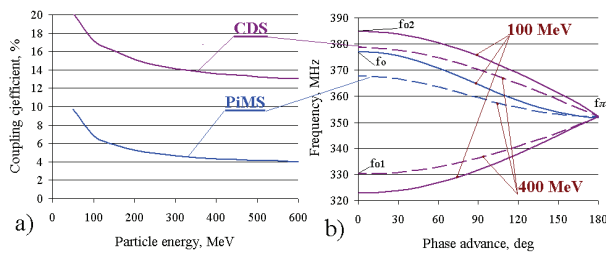


Figure 7: The coupling coefficient  $k_c$  (a) and dispersion curves for PiMs and CDS, (b).

of field at coupling elements. For PiMS there  $k_c$  increasing is possible only at the expense of  $Z_e$  reduction, according to [4]. For CDS  $k_c \approx 14\%$  is realized naturally, just by selecting windows opening to have slots TLT between cells, Fig. 1b. Together with a large  $k_c$ , CDS has the qualitative advantage in the field stability due to intrinsic feature - compensation of perturbations. For low frequency application the cell length  $l_c = \frac{\beta\lambda}{2}$  is relatively large and in structure tank, placed between focusing elements, the number of cells  $N_c \sim (7 \div 11)$  and CDS advantage can be assumed not so bright. But in Fig. 8 are shown the plots for perturbation of  $E_z$  distributions,  $N_c = 7$ , due to tuner insertion to compensate the frequency shift caused by thermal deformations. In Fig. 8 (1) corresponds to reference field distribution without tuners, (2) corresponds to two tuners (T) at the tank ends, inserted to compensate the induced frequency shift and (3) corresponds to a single tuner in the tank middle. Even assuming the open stop band  $\delta f = f_c - f_a \sim 300 \text{ kHz}$ , inserted tuners in CDS do not lead to visible field perturbation and rms deviation is  $\leq 0.5\%$ . For PiMS, tuners, inserted only in end cells, lead to parabolic field perturbation with the maximal range  $\sim 15\%$  and rms deviation  $\sim 5.8\%$ . Such big field perturbation is not tolerable for hadron linac and each PiMS cell is equipped with tuner, [7]. For CDS one or two tuners are sufficient per structure tank. The tuning procedure for CDS also is realized 'in average', avoiding individual cells tuning.

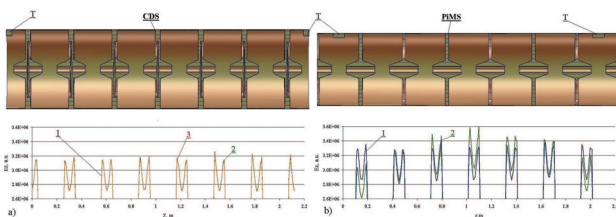


Figure 8: The perturbation of  $E_z$  distributions in tank by tuners (T) insertion to compensate frequency shift caused by thermal deformations.

### Another Properties

The CDS diameter is larger at  $\approx 8\%$ , Fig. 3b. It is not decisive difference. As compared to PiMS, CDS has twice number of transverse webs and welded (or brased) joints. It makes construction more difficult. Tuning procedures are

developed both for CDS, [6], and for PiMS. Tuners in each cell and individual cell tuning are not required in CDS due to higher stability. It simplifies construction. The construction technology for PiMS, [7], can be adapted for CDS. Due to large area of coupling windows, Fig. 1a, PiMS has higher vacuum conductivity. In CDS the main part of residual gas flow comes with slots TLT, Fig. 1b. If required, the area of TLT slots can be increased by windows opening increasing, resulting in a small  $k_c$  increasing and  $Z_e$  reduction and two vacuum ports can be foreseen for CDS tanks.

## SUMMARY

As comparison shows, CDS overcomes PiMS in RF efficiency and, essentially, in the field stability. Attractive CDS features are essential for longer high energy part. CDS construction and tuning looks both more difficult and more easy due to intrinsic properties. For CDS construction the technology, developed for PiMS production, can be adopted. Consideration shows CDS as the perspective candidate for such application.

## REFERENCES

- [1] P. Balleyguier, Coupling Slots Without Shunt Impedance drop. Linac 1996, v.2, p. 414, <http://www.JACoW.org>, 1996
- [2] F. Gerigk et. al., PiMS - a simple and robust accelerating structure for high intensity proton linacs. NIM, A, v. 606, p. 257, 2009
- [3] V. Paramonov, Methods for coupling coefficient increasing in bi-periodical structures. Proc. of the 15-th RuPAC, Protvino, IHEP, v. 1, p. 156, 1996 (in Russian).
- [4] P. Bourquin, et. al., Development status of the Pi Mode Accelerating Structure (PiMs) for Linac 4. Linac 2008, p. 939, <http://www.JACoW.org>, 2008
- [5] V. Paramonov, The Cut Disk Structure Parameters for Medium Proton Energy Range. Linac 2008, p. 910, <http://www.JACoW.org>, 2008
- [6] V. Paramonov et., al, The PITZ CDS Booster Cavity RF Tuning and Start of Conditioning. Linac 2010, p. 241, <http://www.JACoW.org>, 2010
- [7] G. Favre, et. al., Manufacturing of Linac 4 Pi Mode Structure Prototype at CERN, IPAC 2011, p. 1774, <http://www.JACoW.org>, 2011